Fast multilevel radiative transfer

Frédéric Paletou*, Ludovick Léger

Université Paul Sabatier, Toulouse 3, Observatoire Midi-Pyrénées, Laboratoire d'Astrophysique de Toulouse– Tarbes (CNRS/UMR 5572), 14 ave. Edouard Belin, F-31400 Toulouse, France

Abstract

The vast majority of recent advances in the field of numerical radiative transfer relies on approximate operator methods better known in astrophysics as Accelerated Lambda-Iteration (ALI). A superior class of iterative schemes, in term of rates of convergence, such as Gauss–Seidel and successive overrelaxation methods were therefore quite naturally introduced in the field of radiative transfer by Trujillo Bueno and Fabiani Bendicho [A novel iterative scheme for the very fast and accurate solution of non-LTE radiative transfer problems. Astrophys J 1995;455:646]; it was thoroughly described for the non-LTE two-level atom case. We describe hereafter in details how such methods can be generalized when dealing with non-LTE unpolarised radiation transfer with multilevel atomic models, in monodimensional geometry.
© 2006 Elsevier Ltd. All rights reserved.

Keywords: Non-LTE plasmas; Astrophysics; Radiative transfer

1. Introduction

Our ability to deal with complex radiative transfer problems has considerably improved during the last 10 years. It is indeed still worth an effort since important issues of astrophysical interest may require to address a number of cases ranging from multi-dimensional problems in various geometries [2–6] to polarised radiation transfer involving complex atomic models [7,8], for instance.

Most of the recent developments in the field of numerical radiation transfer are based on the approximate (or accelerated) lambda-iteration (ALI) scheme which has been recently reviewed in [9]. ALI methods are based on operator splitting and, in a seminal article, Olson et al. [10] demonstrated the merits of adopting an approximate operator which is nothing more than the exact diagonal of the full operator Λ allowing the determination of the radiation field from a known source function (see [11,12]). More generally speaking such an efficient iterative scheme is better known as the Jacobi's method in numerical analysis [13].

However, even if superior—in term of higher rates of convergence—iterative schemes based on the Gauss–Seidel (GS) and the successive overrelaxation (SOR) methods have been introduced since in the field of numerical radiative transfer, they still deserved too little attention by the astrophysical community. GS/SOR methods have been described in detail in a landmark article [1]; in particular, the practical description of how to implement GS/SOR iterations within a regular short characteristics (SC) formal solver is very meticulously

---

*Corresponding author.

E-mail address: fpaletou@ast.obs-mip.fr (F. Paletou).

written and therefore extremely useful. However, their description of the implementation of GS/SOR methods was restricted to the two-level atom case in monodimensional (1D) geometry.

In a subsequent article [4], although mentions to GS/SOR iterative schemes generalized to the multilevel atom transfer problems can be found, their implementation is far from being made explicit and it is only described in very general terms; it is furthermore embedded in another (very efficient though) numerical strategy based on multi-grid methods [14,15]. Unfortunately, it appears that the basic features of a GS/SOR-based formal solver in the frame of the multilevel atom radiative transfer problem remain, so far, to be made explicit.

The present article aims indeed at filling the gap by providing all the elements required for a successful implementation of *multilevel* GS/SOR iterative schemes in 1D geometry. We shall recall in Section 2 the basic principles of GS/SOR iterative schemes in the case of a two-level atom model. Then, in Section 3 we shall describe step by step how GS/SOR can be implemented for the case of multi-level atom models, therefore extending the well-known multilevel-ALI method of Rybicki and Hummer [16]. Finally, we shall present in Section 4 some illustrative examples clearly demonstrating the performances of multilevel GS/SOR iterative schemes.

2. GS and SOR iterative schemes basics

GS and SOR iterative scheme are particularly well adapted to the SC method for the formal solution of the radiative transfer equation [2,17,18].

Using SC in 1D geometry indeed, the formal solution is obtained by sweeping the grid say, first in direction $-\Omega$ ($\mu < 0$) i.e. from the surface down to the bottom of the atmosphere, and then in the opposite, upward direction $+\Omega$ ($\mu > 0$) starting from the bottom of the atmosphere up to its surface though. The specific intensity $I_{\nu\Omega}$ is advanced step by step during each pass, partially integrated over angles and frequencies during the downward pass while, during the second (upward) pass, the mean intensity $\bar{J}$ can be fully computed, completing therefore the formal solution at each depth

$$\bar{J}_k = \Lambda[S_k]. \tag{1}$$

Except at the boundaries where the illumination conditions are known a priori, along each direction, the specific intensity at the inner grid points is advanced depth after depth, and computed along the SC (allowing us to suppress any index related to the angle variation of the specific intensity hereafter) according to

$$I_o = I_u e^{-\Delta\tau_u} + \Psi_u S_u + \Psi_o S_o + \Psi_d S_d, \tag{2}$$

where the first part of the right-hand side of this expression corresponds to the part transmitted from the "upwind" grid point u down to the current point o (see Fig. 1), and the three last terms result from the analytic integration of

$$\Upsilon = \int_0^{\Delta\tau_u} S(\tau) e^{-\tau}\, d\tau \tag{3}$$

along the SC going from u to o. Indeed, assuming that S is quadratic in the optical depth τ, it is easy to show, using a simple Lagrange polynomial interpolation on the basis of three consecutive grid points u, o and d, that

$$\Upsilon = \Psi_u S_u + \Psi_o S_o + \Psi_d S_d, \tag{4}$$

where the Ψ's coefficients are defined[1] as

$$\begin{cases} \Psi_u = \dfrac{w_2 + w_1 \Delta\tau_d}{\Delta\tau_u(\Delta\tau_u + \Delta\tau_d)}, \\[2ex] \Psi_o = w_0 + \dfrac{w_1(\Delta\tau_u - \Delta\tau_d) - w_2}{\Delta\tau_u \Delta\tau_d}, \\[2ex] \Psi_d = \dfrac{w_2 - w_1 \Delta\tau_u}{\Delta\tau_d(\Delta\tau_u + \Delta\tau_d)}, \end{cases} \tag{5}$$

---

[1] A different expression was used in [2], Eqs. (8)–(10); note also that there is a sign error in their coefficients d_1 and d_2. But more important is to adopt the current expansion in terms of Ψ's for the efficient implementation of GS/SOR.
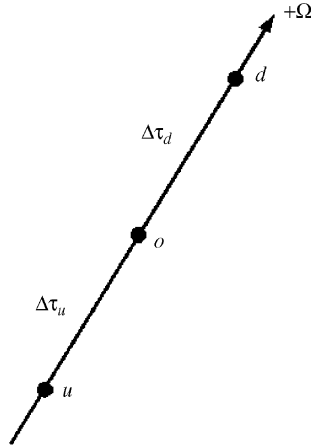
Fig. 1. Three successive grid points along direction $+\Omega$ (upward) are used, assuming parabolic interpolation of the source function, in order to compute the specific intensity at current position o along the short characteristics starting from u.

and where

$$\begin{cases} w_0 = 1 - e^{-\Delta\tau_u}, \\ w_1 = w_0 - \Delta\tau_u e^{-\Delta\tau_u}, \\ w_2 = 2w_1 - \Delta\tau_u^2 e^{-\Delta\tau_u}. \end{cases} \tag{6}$$

In the *two-level atom case*, the non-LTE line source function S is usually expressed as

$$S(\tau) = (1 - \varepsilon)\bar{J}(\tau) + \varepsilon B(\tau), \tag{7}$$

where τ is the optical depth, ε is the collisional destruction probability measuring departures from LTE, B the Planck function and $\bar{J}$ is the usual mean intensity

$$\bar{J} = \int \frac{d\Omega}{4\pi} \int \phi_\nu I_{\nu\Omega}\, d\nu, \tag{8}$$

where we omitted the optical depth dependence for simplicity.

The Jacobi type iterative scheme introduced in numerical radiative transfer by [10] allows for the iterative determination of the source function on the basis of increments such that

$$\Delta S_k = \frac{(1 - \varepsilon)\bar{J}_k^{(\text{old})} + \varepsilon B_k - S_k^{(\text{old})}}{1 - (1 - \varepsilon)\Lambda_{kk}}, \tag{9}$$

at each depth τ_k, where the superscript (old) denotes quantities already known from the previous iterative stage and where Λ_{kk} is a *scalar* equal to the diagonal element of the full operator Λ at such a depth in the atmosphere.

Within a GS iterative scheme the source function increments now turn themselves into

$$\Delta S_k^{(\text{GS})} = \frac{(1 - \varepsilon)\bar{J}_k^{(\text{old and new})} + \varepsilon B_k - S_k^{(\text{old})}}{1 - (1 - \varepsilon)\Lambda_{kk}}, \tag{10}$$

where the somewhat enigmatic quantity $\bar{J}_k^{(\text{old and new})}$ means that at the spatial point k the mean intensity has to be calculated via a formal solution of the transfer equation using the "new" source function values $S_j^{(\text{new})}$ already obtained at points $j = 1, 2, \ldots, (k-1)$, and the "old" source function values $S_j^{(\text{old})}$ at points $j = k, (k+1), \ldots, \text{ND}$.

Achieving this was explained in every detail in [1] and we shall not repeat here the algorithmics of the process. It is however important to repeat that such a scheme is better implemented in the frame of the SC approach since it allows to avoid any explicit matrix inversion.

Finally, going beyond GS, SOR iterations can be implemented where

$$\Delta S_k^{(\text{SOR})} = \omega \Delta S_k^{(\text{GS})}, \tag{11}$$

ω being, in the case of *overrelaxation*, a parameter such that $1 < \omega < 2$, with an optimal value ~ 1.5 for the two-level atom case [1].

However, in the non-LTE multilevel atom case, the radiation transfer problem is somewhat more complicated since it is now required to solve *self-consistently* for the coupled set of N_{trans} radiative transfer equations, for all radiatively allowed transitions, together with a set of N_{levels} equations of the statistical equilibrium (ESE) *at each optical depth* giving the populations numbers for all atomic levels.

3. The multilevel atom case

Hereafter, we shall describe in detail how the GS/SOR numerical method can be implemented for the case of multilevel atom models in 1D geometry. For simplicity we shall consider the case of non-overlapping lines with no background continuum.

3.1. The MALI method: an overview

ALI methods have been first generalized to the multilevel atom case by Rybicky and Hummer [16,19]. Their MALI method consists in the *preconditioning* of the ESE using an approximate operator $\bar{\Lambda}_{ul}^*$ and a $\bar{J}_{ul}^{\text{eff}}$ mean intensity defined hereafter, and computed, for all allowed transitions $u \leftrightarrow l$, from quantities known from the previous iterative step.

Generally speaking, the line source function for a radiative transition between the two bound atomic levels u (i.e., the upper energy level) and l (respectively, the lower one) can be written in terms of the density of populations $n_{u,l}$, the Einstein [20] coefficients for spontaneous emission A_{ul}, absorption B_{lu} and stimulated emission B_{ul}, and the line absorption ϕ_v and emission ψ_v profiles such as

$$S_{ul}(v) = \frac{n_u A_{ul} \psi_v}{n_l B_{lu} \phi_v - n_u B_{ul} \psi_v}. \tag{12}$$

Hereafter, we shall however restrict our study to complete redistribution in frequency for which absorption and emission profiles are identical, i.e. $\phi_v \equiv \psi_v$ and therefore, the line source function remains *independent* of the frequency. It is indeed well-known that such an assumption remains valid for most of the spectral lines; however, partial redistribution in frequency effects should be considered, at the cost of more computational work, for a proper description of resonance line formation in a diluted medium (e.g., [21] and references therein).

Furthermore, leaving out bound-free transitions, at each depth in the atmosphere, the ESE are usually expressed as a set of N_{levels} elementary equations such that

$$\sum_{j<i} [n_i A_{ij} - (n_j B_{ji} - n_i B_{ij}) \bar{J}_{ij}] - \sum_{j>i} [n_j A_{ji} - (n_i B_{ij} - n_j B_{ji}) \bar{J}_{ij}] + \sum_j (n_i C_{ij} - n_j C_{ji}) = 0, \tag{13}$$

where the C_{ij} are collisional excitation/deexcitation rates. Now, introducing the approximate operator into the ESE via the ALI approximation

$$I_{v\Omega} \simeq \Lambda_{v\Omega}^*[S] + (\Lambda_{v\Omega} - \Lambda_{v\Omega}^*)[S^{(\text{old})}], \tag{14}$$

where $S^{(\text{old})}$ represents the source function known from previous iteration and, defining

$$\begin{cases} \bar{J}_{ij} \simeq \int \frac{\mathrm{d}\Omega}{4\pi} \int \phi_v \Lambda_{v\Omega}^*[S] \, \mathrm{d}v + \bar{J}_{ij}^{\text{eff}}, \\ \bar{J}_{ij}^{\text{eff}} = \int \frac{\mathrm{d}\Omega}{4\pi} \int \phi_v (\Lambda_{v\Omega} - \Lambda_{v\Omega}^*)[S^{(\text{old})}] \, \mathrm{d}v, \end{cases} \tag{15}$$

where $\bar{J}_{ij}^{\mathrm{eff}}$ depends only on known quantities, we can establish[2] after [16] the following set of preconditioned equations

$$\sum_{j<i}[n_i A_{ij}(1-\bar{A}_{ij}^*)-(n_j B_{ji}-n_i B_{ij})\bar{J}_{ij}^{\mathrm{eff}}] - \sum_{j>i}[n_j A_{ji}(1-\bar{A}_{ij}^*)-(n_i B_{ij}-n_j B_{ij})\bar{J}_{ij}^{\mathrm{eff}}]$$
$$+\sum_{j}(n_i C_{ij}-n_j C_{ji})=0, \tag{16}$$

where

$$\bar{A}_{ij}^* = \int \frac{\mathrm{d}\Omega}{4\pi}\int \phi_v A_{v\Omega}^* \,\mathrm{d}v. \tag{17}$$

Heinzel [22] and Paletou [21] showed how to take care self-consistently of the ionization equilibrium within the MALI approach by adding a Newton–Raphson scheme to it, for the determination of the electron density from a set of non-linear ESE taking into account all kind of bound-free transitions; the same can be done within the new GS/SOR multilevel numerical schemes.

3.2. Expliciting GS/SOR with multilevel atoms

Assume that one has *already* swept the grid *once*, say from the illumination-free surface of the atmosphere at $k=0$, down to the bottom boundary at $k=\mathrm{ND}$ along direction $-\Omega$. By analogy with the GS/SOR numerical strategy for the two-level atom case, in the multilevel atom case we are now going to update all population numbers at successive depths $k=\mathrm{ND},\ldots,1$ *while sweeping back the grid along the opposite, upward direction* $+\Omega$.

Now the population update will be made depth after depth, from the bottom, up to the surface of the atmosphere by inverting the MALI preconditioned set of ESE given in Eq. (16) *before* passing to the next depth point. It is a quite straightforward task at the lower boundary surface since the incident radiation field is known a priori from the (given) external conditions of illumination.

The situation is however a bit more tricky at the inner grid points. Once the populations at depth $(k+1)$ have been updated, we shall advance along direction $+\Omega$ to the next grid point at depth k. But having changed $\{n_j^{(\mathrm{old})}\}_{(k+1)}$ to $\{n_j^{(\mathrm{new})}\}_{(k+1)}$ means that the local absorption coefficients $\chi_{(k+1)}$ *and* the source functions for all allowed transitions have to be changed accordingly, as well as the upwind optical depth $\Delta\tau_{(k+1)}^{(\uparrow)}$ along the path from depth $(k+1)$ to depth k. As a consequence, the three coefficients $\Psi_d^{(\uparrow)}$ $[d=(k-1),k,(k+1)]$ used for the evaluation of the specific intensity along the SC are also affected by the local population change and thus need to be updated. But since $\Delta\tau_{(k+1)}^{(\uparrow)}=\Delta\tau_{(k-1)}^{(\downarrow)}$ evaluations of the specific intensities made during the first downward pass must also be corrected accordingly, for consistency.

So the major point in such implementation is to carefully "propagate" the effects of the local population update. Let us, for instance, consider the specific intensity evaluation at any inner grid point k in, respectively, direction $-\Omega$ for which we shall use $(\downarrow)$ superscripts, and $+\Omega$ (resp. $(\uparrow)$ superscripts); we can therefore write, following Eq. (2)

$$I_k^{(\downarrow)} = I_{k-1}^{(\downarrow)}\mathrm{e}^{-\Delta\tau_{(k-1)}^{(\downarrow)}} + \Psi_{k-1}^{(\downarrow)}S_{k-1} + \Psi_k^{(\downarrow)}S_k + \Psi_{k+1}^{(\downarrow)}S_{k+1}, \tag{18}$$

while, at the same depth but in the opposite direction, we have

$$I_k^{(\uparrow)} = I_{k+1}^{(\uparrow)}\mathrm{e}^{-\Delta\tau_{(k+1)}^{(\uparrow)}} + \Psi_{k+1}^{(\uparrow)}S_{k+1} + \Psi_k^{(\uparrow)}S_k + \Psi_{k-1}^{(\uparrow)}S_{k-1}. \tag{19}$$

Since the update of the population numbers at depth $(k+1)$ have just been done by inverting the system of Eq. (16), this generates *for each allowed transition* changes in the absorption coefficients at line center, now becoming

$$\chi_{(k+1)}^{(\mathrm{new})} = \left(\frac{h v_{ul}}{4\pi}\right)[n_l^{(\mathrm{new})}B_{lu}-n_u^{(\mathrm{new})}B_{ul}] \tag{20}$$

---

[2]Inserting Eq. (12) into Eq. (14) and forming the net radiative rate $(n_j B_{ji}-n_i B_{ij})\bar{J}_{ij}$ in terms of $\bar{A}_{ij}^*$ and $\bar{J}_{ij}^{\mathrm{eff}}$.

and in the line source functions, assuming complete redistribution in frequency, turning into

$$S^{(\text{new})}_{(k+1)} = \frac{n^{(\text{new})}_u A_{ul}}{n^{(\text{new})}_l B_{lu} - n^{(\text{new})}_u B_{ul}}. \tag{21}$$

Therefore, one has first to correct $I^{(\downarrow)}_k$ for consistency since previous changes lead, according to Eq. (18), to

$$I^{(\downarrow),\,(\text{new})}_k = I^{(\downarrow),\,(\text{old})}_{k-1} e^{-\Delta\tau^{(\downarrow),\,(\text{old})}_{(k-1)}} + \Psi^{(\downarrow),\,(\text{new})}_{k-1} S^{(\text{old})}_{k-1} + \Psi^{(\downarrow),\,(\text{new})}_k S^{(\text{old})}_k + \Psi^{(\downarrow),\,(\text{new})}_{k+1} S^{(\text{new})}_{k+1}, \tag{22}$$

which requires that $I^{(\downarrow),\,(\text{old})}_{k-1}$ have been saved in memory during the first downward pass. This step is equivalent to the computation of the ΔJ^{in}_k correction pointed out in [1], Eq. (39).

Then, $I^{(\uparrow)}_k$ can be computed in a straightforward manner via Eq. (19), which makes it possible to compute $\bar{\Lambda}^*_{ij}$ and $\bar{J}^{\text{eff}}_{ij}$ for all allowed transitions, then to inject these quantities in the preconditioned ESE and finally to compute/update locally $\{n^{(\text{new})}_j\}_k$ while in the middle of the upward pass.

However, before advancing to next depth point $(k-1)$, it is important to consider first the various changes induced by the level population changes, respectively, on the source functions S_k, on the optical depth increments $\Delta\tau^{(\uparrow),\,(\text{new})}_{(k+1)}$ and $\Delta\tau^{(\uparrow),\,(\text{new})}_{(k-1)}$ as well as, finally, on the three SC coefficients $\Psi^{(\uparrow)}_d$ [$d = (k-1)$, k, $(k+1)$]. Because of that, we end up all updates at depth k during the upward pass by the computation of

$$I^{(\uparrow),\,(\text{new})}_k = I^{(\uparrow)}_{k+1} e^{-\Delta\tau^{(\uparrow),\,(\text{new})}_{(k+1)}} + \Psi^{(\uparrow),\,(\text{new})}_{k+1} S^{(\text{new})}_{k+1} + \Psi^{(\uparrow),\,(\text{new})}_k S^{(\text{new})}_k + \Psi^{(\uparrow),\,(\text{new})}_{k-1} S^{(\text{old})}_{k-1}. \tag{23}$$

This last stage is analogous to the correction described by Eq. (40) in [1].

Finally, a multilevel SOR iterative scheme is built when, at each depth k, all the populations of the excited levels are updated according to

$$n^{(\text{new})}_k = n^{(\text{old})}_k + \omega\Delta n^{(\text{GS})}_k, \tag{24}$$

where ω is a parameter of the order of 1.5 as discussed below.

3.3. Numerical recipes

Several "recipes" should be followed when implementing a GS/SOR solver for multilevel atoms. The first one is to order properly the various loops. From outer to inner loops one may find indeed: (1) the directions ($\pm\Omega$) along which the slab will be swept, (2) the number of allowed radiative transitions, (3) the direction cosines (i.e., the usual μ's) and, finally (4) the frequencies.

Upwind and downwind corrections, as described in Eqs. (22) and (23), require some bookkeeping of variables such as all the $I^{(\downarrow),\,(\text{old})}_k$ after the downwind pass $-\Omega$ for the further computation of the mean intensity entering the preconditioned ESE i.e., Eq. (16).

Finally, it is important to realize that the additional computing time necessary for all the extra-computations required by one GS/SOR iterative step is very small as compared to the huge saving on the whole convergence process with respect to MALI (see Table 1).

4. Illustrative examples and discussion

We have adopted the standard benchmark models for multilevel atom problems proposed by Avrett [23] and Avrett and Loeser [24] whose main parameters have also been summarized in Table 2.

The respective rates of convergence for the MALI, GS and SOR multilevel iterative processes are displayed in Fig. 2 where we plotted the maximum relative change on the level populations from an iteration to another, R_c, for the schematic 3-level H I model. A spatial grid of 20 depth points per decade together with a 8 Gauss–Legendre angular quadrature and constant Doppler profiles were used. It clearly demonstrates how superior to MALI the multilevel SOR iterative scheme can be for such refined grids; and it is worth pointing out here again the importance of grid refinement on the accuracy of ALI-class methods, as demonstrated by Chevallier et al. [25]. Indeed, in such a case a factor of ~6 in computing time can be saved, when one iterates the population numbers down to numerical noise, for instance. We report a similar behaviour of the iterative processes when dealing with Avrett's Ca II ion model.

Table 1

Computation time for the 3-level H model of [23] obtained with an Intel Pentium-4 clocking at 3 GHz as a function of the number of depth points per decade N_τ; the stopping criterion was $R_c = 10^{-10}$ (we also indicate the # of iterations required, respectively)

N_τ	MALI	GS	SOR
5	7.644 s (160)	4.595 s (78)	2.325 s (39)
10	27.852 s (326)	17.148 s (161)	6.096 s (55)
15	59.768 s (483)	38.997 s (239)	10.203 s (63)
20	1 min 43.373 s (634)	1 min 05.879 s (315)	17.213 s (81)
25	2 min 37.637 s (780)	1 min 40.630 s (387)	26.040 s (99)

Table 2

Input parameters for the H I and Ca II multilevel benchmark models of Avrett [23]. Statistical weights are $g_1 = 2$, $g_2 = 8$, and $g_3 = 18$ for H I, $g_1 = 2$, $g_2 = 4$, $g_3 = 6$, $g_4 = 2$, $g_5 = 4$ for Ca II; the temperature of the atmosphere is 5000 K

Element	u	l	A_{ul}	C_{ul}	v_{ul}
H	2	1	4.68×10^8	10^5	2.47×10^{15}
H	3	1	5.54×10^7	10^5	2.93×10^{15}
H	3	2	4.39×10^7	10^5	–
Ca	2	1	Forbidden	8.2×10^3	4.10×10^{14}
Ca	3	1	Forbidden	8.2×10^3	4.12×10^{14}
Ca	4	1	1.4×10^8	5.1×10^4	7.56×10^{14}
Ca	5	1	1.4×10^8	5.1×10^4	7.63×10^{14}
Ca	3	2	Forbidden	10^7	–
Ca	4	2	7.8×10^6	1.6×10^5	–
Ca	5	2	8.1×10^5	1.6×10^4	–
Ca	4	3	Forbidden	10^3	–
Ca	5	3	7.2×10^6	1.4×10^5	–
Ca	5	4	Forbidden	4.8×10^6	–

In Fig. 3, we display (solid lines) the source function vs. line optical depth for the three transitions allowed by our schematic H-model. Dashed lines correspond to the old benchmark results of [23]; differences are coming not only from very different numerical schemes but also from large differences in the angular and frequency quadratures. Our results are also in good agreement with those of [26] and may serve, given the high-level of grid refinement we adopted, as new benchmark results for multilevel atom cases.

The main potential drawback of SOR methods is that it relies on the choice of a relaxation parameter ω whose optimal value is a priori unknown. However, it was proposed [1] a quite robust numerical procedure in order to estimate *self-consistently* a close-to-optimal ω after having run a few "pure GS" iterations. We followed their recommendations and, indeed, found a posteriori values close to "optimal" ones deduced from experimental runs using a prescribed ω.

Finally, in Fig. 4, we plotted the history of the convergence error C_e defined as

$$C_e = \max\left(\frac{|n(itr) - n(\infty)|}{n(\infty)}\right), \tag{25}$$

following [3], where *itr* is the iteration number and $n(\infty)$ is the fully converged solution, and of the relative change R_c for, respectively, the GS and the SOR multilevel iterative schemes. It is important to note again that reaching a small value of R_c, which is indeed the most direct control parameter of the iterative process, does *not* necessarily imply a small enough value of C_e to guarantee convergence; and this is shown by the GS
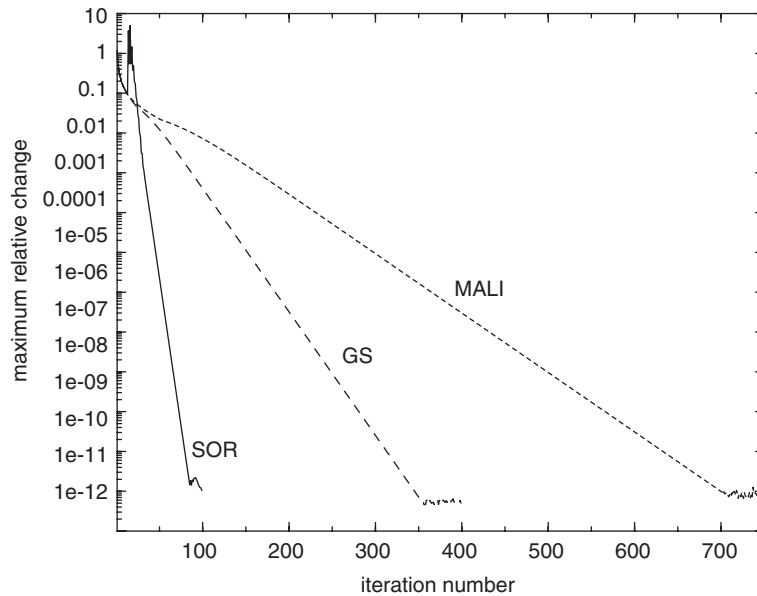
Fig. 2. Rates of convergence for the MALI, Gauss–Seidel and SOR multilevel iterative processes, respectively. A spatial grid of 20 depth points per decade together with a 8 Gauss–Legendre angular quadrature and constant Doppler profiles were used. The atomic model is a 3-level H I model atom taken from [23] (see also Table 2).
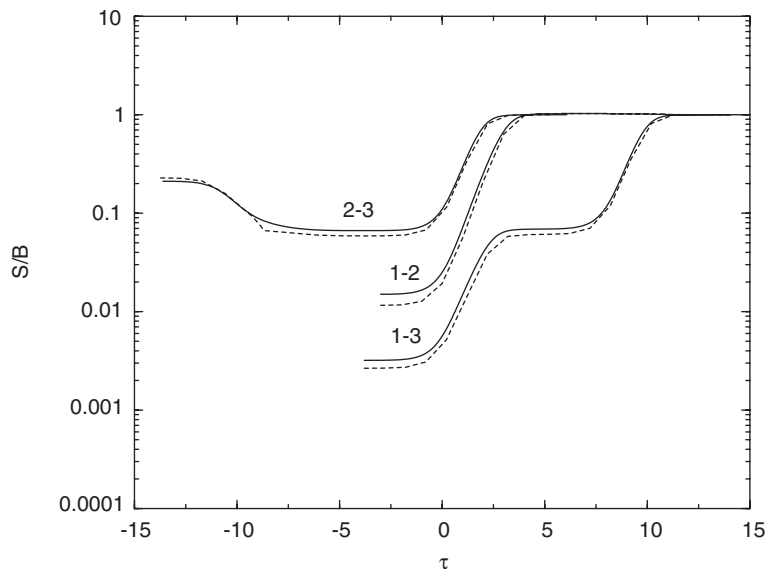

Fig. 3. Source functions vs. optical depth for the three transitions of our H-model. Solid lines are our GS/SOR multilevel results and dashed lines correspond to low-resolution results previously published in [23,26].

curves. However, an optimal SOR iterative process including the self-consistent evaluation of ω as proposed in [1], leads to a better-controlled process since R_c is just slightly lower than C_e, as shown in Fig. 4.

The issue of having a reliable stopping criterion is of course critical to any iterative method and, for the specific case of numerical radiative transfer, Auer et al. [3] and Fabiani Bendicho et al. [4] addressed it successfully by adopting *multi-grid* methods. We finally refer the reader to this later work where it is
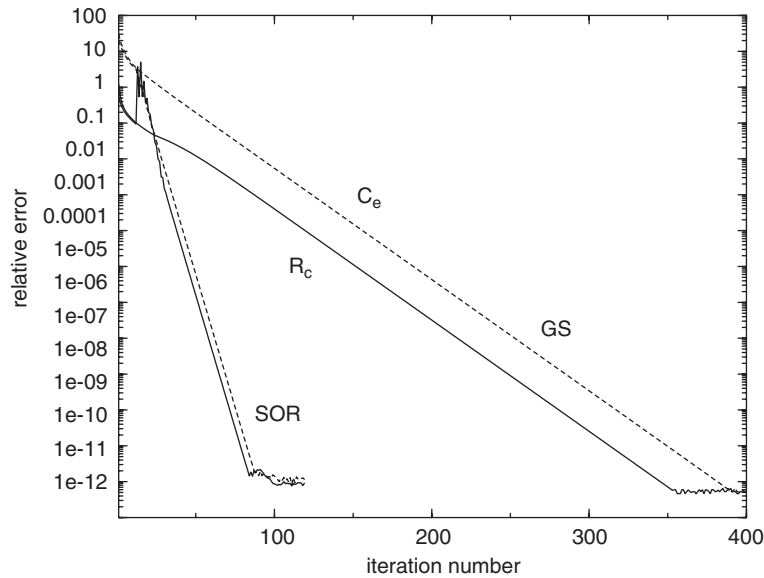
Fig. 4. History of the convergence error C_e (dashed lines) and of the relative change R_c (full lines) for, respectively, the GS and the SOR multilevel iterative schemes. Although a small value of R_c does not necessarily imply a small enough value of C_e as demonstrated by the GS curves, a SOR iterative process including a self-consistent evaluation of ω leads to a scheme such that $R_c \simeq C_e$.

demonstrated how the *combination* of GS/SOR iterative schemes together with multi-grid techniques lead to extremely powerful techniques for the solution of complex radiative transfer problems.

Acknowledgments

References

[1] Trujillo Bueno J, Fabiani Bendicho P. A novel iterative scheme for the very fast and accurate solution of non-LTE radiative transfer problems. Astrophys J 1995;455:646.

[2] Auer LH, Paletou F. Two-dimensional radiative transfer with partial frequency redistribution I. General method. Astron Astrophys 1994;285:675.

[3] Auer LH, Fabiani Bendicho P, Trujillo Bueno J. Multidimensional radiative transfer with multilevel atoms. I. ALI method with preconditioning of the rate equations. Astron Astrophys 1994;292:599.

[4] Fabiani Bendicho P, Trujillo Bueno J, Auer LH. Multidimensional radiative transfer with multilevel atoms. II. The non-linear multigrid method. Astron Astrophys 1997;324:161.

[5] van Noort M, Hubeny I, Lanz T. Multidimensional non-LTE radiative transfer. I. A universal two-dimensional short-characteristics scheme for cartesian, spherical, and cylindrical coordinate systems. Astrophys J 2002;568:1066.

[6] Gouttebroze P. Radiative transfer in cylindrical threads with incident radiation. Astron Astrophys 2004;413:733.

[7] Trujillo Bueno J, Manso Sainz R. Iterative methods for the non-LTE transfer of polarized radiation: resonance line polarization in one-dimensional atmospheres. Astrophys J 1999;516:436.

[8] Trujillo Bueno J. In: Hubeny I, Mihalas D, Werner K, editors. ASP conference series, Stellar atmosphere modeling, vol. 288. San Francisco: Astronomical Society of the Pacific; 2003. p. 551.

[9] Hubeny I. In: Hubeny I, Mihalas D, Werner K, editors. ASP conference series, Stellar atmosphere modeling, vol. 288. San Francisco: Astronomical Society of the Pacific; 2003. p. 17.

[10] Olson GL, Auer LH, Buchler JR. A rapidly convergent iterative solution of the non-LTE line radiation transfer problem. JQSRT 1986;35:431.

[11] Mihalas D. Stellar atmospheres. San Francisco: Freeman; 1978.

[12] Rutten RJ. In: Hubeny I, Mihalas D, Werner K, editors. ASP conference series, Stellar atmosphere modeling, vol. 288. San Francisco: Astronomical Society of the Pacific; 2003. p. 99 (see also Radiative Transfer in Stellar Atmospheres, Sterrekunding Instituut Utrecht ⟨http://www.fys.ruu.nl/~rutten/Astronomy_course.html⟩).

[13] Young DM. Iterative solution of large linear systems. New York: Academic Press; 1971.

[14] Hackbusch W. Multi-grid methods and applications. Berlin: Springer; 1985.

[15] Briggs WL, Henson VE, McCormick SF. A multigrid tutorial. Philadelphia, PA: SIAM; 2000.

[16] Rybicki GB, Hummer DG. An accelerated lambda iteration method for multilevel radiative transfer. I. Non-overlapping lines with background continuum. Astron Astrophys 1991;245:171.

[17] Olson GL, Kunasz PB. Short characteristic solution of the non-LTE line transfer problem by operator perturbation. I. The one-dimensional planar slab. JQSRT 1987;38:325.

[18] Kunasz PB, Auer LH. Short characteristic integration of radiative transfer problems—formal solution in two-dimensional slabs. JQSRT 1988;39:67.

[19] Rybicki GB, Hummer DG. An accelerated lambda iteration method for multilevel radiative transfer. II. Overlapping transitions with full continuum. Astron Astrophys 1992;262:209.

[20] Einstein A. Zur quantentheorie der strahlung. Phys Z 1917;18:121.

[21] Paletou F. Two-dimensional multilevel radiative transfer with standard partial frequency redistribution in isolated solar atmospheric structures. Astron Astrophys 1995;302:587.

[22] Heinzel P. Multilevel NLTE radiative transfer in isolated atmospheric structures: implementation of the MALI-technique. Astron Astrophys 1995;299:563.

[23] Avrett EH. In: Athay RG, Mathis J, Skumanich A, editors. Resonance lines in astrophysics, National Center for Atmospheric Research, Boulder; 1968. p. 27.

[24] Avrett EH, Loeser R. In: Kalkofen W, editor. Numerical radiative transfer. Cambridge: Cambridge University Press; 1987. p. 135.

[25] Chevallier L, Paletou F, Rutily B. On the accuracy of the ALI method for solving the radiative transfer equation. Astron Astrophys 2003;411:221.

[26] Atanacković-Vukmanović O, Crivellari L, Simonneau E. A forth-and-back implicit Λ-iteration. Astrophys J 1997;487:735.